

CONCLUSION

With the newly measured values of the cross sections for production of Ge^{77m} and Ge^{77} ,⁶ the one exception to

⁶ Our Ge^{76} thermal neutron activation cross sections are close to older values reported by Seren, Friedlander, and Turkel, U. S. Atomic Energy Commission Report MDDC-408 (unpublished), and J. R. Arnold and N. Sugarman, J. Chem. Phys. **15**, 703 (1947), who give 0.085 barn for production of the 12-hr activity and state that the cross section for the 59-sec activity is 10% higher than that for the 12-hr activity. A new measurement of these cross sections has also been reported by W. S. Lyon and J. S. Eldridge, Phys. Rev. **107**, 1056 (1957) who give 0.14 barn and 0.043 barn for the production of Ge^{77m} and Ge^{77} , respectively, by pile neutrons.

the isomeric ratio rule is removed. Again referring to Fig. 1, we see that the point for Ge^{77} calculated on the basis of our new measurements of the cross sections for production of Ge^{77} and Ge^{77m} , falls just to the right of the 0.5 line.

ACKNOWLEDGMENT

The authors wish to express their appreciation to David Larsen for his assistance in obtaining some of the data in this paper.

Although these values are considerably different from our values, they, too, are in agreement with the isomeric ratio rule.

Coincidence Studies of the $\text{Ni}^{58}(p,2p)$ Reaction

BERNARD L. COHEN

Oak Ridge National Laboratory,* Oak Ridge, Tennessee

(Received July 18, 1957)

The $\text{Ni}^{58}(p,2p)$ reaction, by far the predominant reaction in that nucleus, was studied by detecting the two outgoing protons in coincidence. Measurements were made of the energy spectra of all protons from the reaction, of the spectrum of the sum of the energies of the two outgoing protons, and of the angular correlations of the outgoing protons with each other and with the incident proton. The results indicate quite conclusively that the preponderance of $(p,2p)$ over (p,pn) reactions in Ni^{58} is not due to the relative level densities of the final nuclei, the ineffectiveness of Coulomb barriers, or a high emission energy of the "first" proton leaving emission of a neutron energetically forbidden. Other possible explanations are considered.

There is strong evidence that the $(p,2p)$ reaction mechanism is predominantly a direct one in which the two protons are "knocked-out" simultaneously.

INTRODUCTION

AMONG the strangest anomalies in the field of medium-energy nuclear reactions are the very large (x,pn) and $(x,2p)$ cross sections in medium-weight elements.¹⁻³ For example, with a 23-Mev bombarding energy, (p,pn) reactions have far larger cross sections than $(p,2n)$ reactions in all elements lighter than zinc,¹ and in many cases, the heaviest example of which is Ni^{58} , the most probable reaction is $(p,2p)$.² There has been much speculation¹⁻⁴ on the explanation for these effects, but the theoretical analysis of total cross sections is too tenuous to allow positive conclusions to be reached. To obtain a deeper experimental hold on the problem, an investigation of the $\text{Ni}^{58}(p,2p)$ reaction was undertaken by coincidence detection of the outgoing protons. Angular correlations between these, and between them and the incident proton were studied.

All measurements were made as a function of the energy of each of the two outgoing protons, and as a function of the sum of their energies.

To review the situation, the energetic thresholds for the various reactions in Ni^{58} are listed in Table I. The known excited states of Co^{57} are at 1.38, 1.50, and 1.91 Mev. The observed cross sections are 240 mb for the sum of the $(p,pn) + (p,2n) + (p,np) + (p,d)$ reactions,

* Operated for the U. S. Atomic Energy Commission by Union Carbide Nuclear Company.

¹ B. L. Cohen and E. Newman, Phys. Rev. **99**, 718 (1955).

² Cohen, Newman, and Handley, Phys. Rev. **99**, 723 (1955).

³ Miller, Friedlander, and Markowitz, Phys. Rev. **98**, 1197(A) (1955); J. M. Miller, and F. S. Houck, Bull. Am. Phys. Soc. Ser. II, **2**, 60 (1957); S. N. Ghoshal, Phys. Rev. **80**, 939 (1950).

⁴ J. M. Blatt and V. F. Weisskopf, *Theoretical Nuclear Physics* (John Wiley and Sons, Inc., New York, 1952), p. 494; also, 1955 Gordon Conference on Nuclear Chemistry (unpublished).

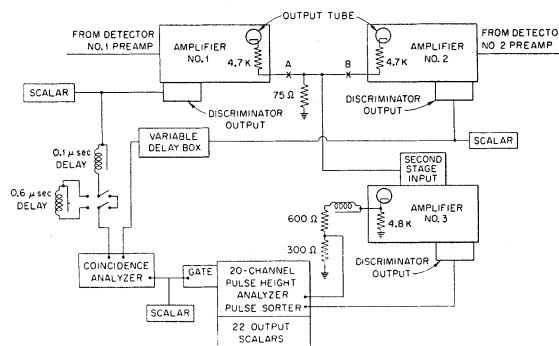


FIG. 1. Electronic circuitry for measuring distribution of sum of pulse heights of coincidence pulses. By breaking the connection at B (or A), the pulse-height distribution of pulses in detector No. 1 (or No. 2) in coincidence with pulses from the other detector is measured.

vs 680 mb for the (*p*, 2*p*) reaction.² For purpose of the discussion, the ratio of $\sigma(p, 2p)/\sigma(p, pn)$ is important. In view of the measurements, it is conservatively assumed that this ratio is a factor of four.

EXPERIMENTAL

The apparatus consists essentially of a scattering chamber with two detectors for the reaction products; a coincidence between the two detectors signals a (*p*, 2*p*) reaction. Gating with this coincidence, measurements are made of the pulse-height distribution in one of the two detectors and of the distribution of the sum of the pulse heights in the two detectors. These measurements are made for various angular positions of the two detectors relative to the incident beam on both the left and right side of the latter. The 23-Mev proton beam from the ORNL 86-inch cyclotron passes through a $\frac{1}{8}$ -in. diameter collimating slit into a 4-in. diameter scattering chamber, through a thin target located at its center, and thence into a Faraday cup which measures the integrated beam. One-inch high windows of 1-mil Mylar extend from 15° to 165° around the

TABLE I. Energetic thresholds for proton-induced reactions in Ni⁵⁸

Reaction	Energetic thresholds (Mev)
Ni ⁵⁸ (<i>p</i> , <i>p</i>)Ni ⁵⁸	0
Ni ⁵⁸ (<i>p</i> , <i>n</i>)Cu ⁵⁸	9
Ni ⁵⁸ (<i>p</i> , 2 <i>n</i>)Cu ⁵⁷	20.6
Ni ⁵⁸ (<i>p</i> , <i>pn</i>)Ni ⁵⁷	11.9
Ni ⁵⁸ (<i>p</i> , 2 <i>p</i>)Cu ⁵⁷	8.0

periphery of the scattering chamber on both its left and right sides. The detectors, 1-in. diameter by $\frac{1}{8}$ -in. thick NaI(Tl) crystals connected by 1-in. long Lucite light pipes to Dumont 6291 photomultipliers, are positioned against these windows. The crystals are covered with $\frac{1}{4}$ -mil aluminum-coated Mylar films which serve as reflectors and also as a seal for light and moisture.

The target holder contains three targets; it is mounted on a shaft which passes out of the scattering chamber lid through an O-ring seal. This allows any of the three targets to be placed in the beam, and the target angle to be rotated without breaking the vacuum. The three targets are a phosphorescent foil for observing the position of the beam, and thus aligning the chamber, a 2.5-mg/cm² nickel foil which is used as the principal target, and a thin polyethylene target for calibrations using the kinematically required coincidence from proton-proton scattering. The beam is monitored by a scintillation detector viewing the target at an angle of about 20° through a small window out of the detector plane. This proved slightly more reliable than the Faraday cup, and in addition takes into account the angle of the target to the beam.

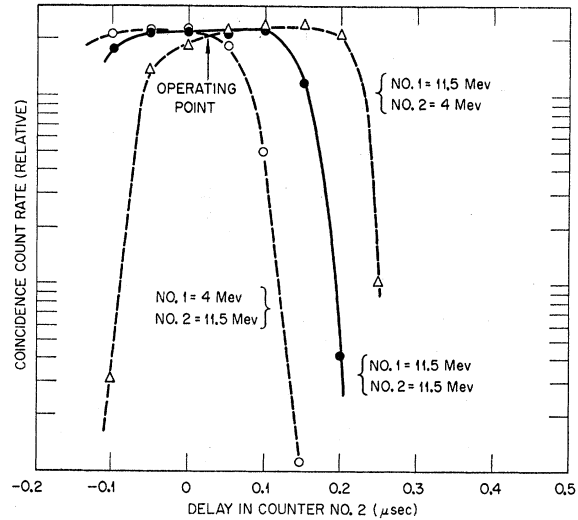


FIG. 2. Time-resolution curves obtained with *p*-*p* scattering from a polyethylene target. Detectors are at 45°L and 45°R. Reduced energies are obtained with absorbers.

The circuitry consists of three *A*-1-*D* amplifiers,⁵ an ORNL-type 0.1- μ sec resolving-time coincidence analyzer, and a 20-channel pulse-height analyzer; the arrangement is shown schematically in Fig. 1. The pulses from the two photomultipliers are passed through amplifiers No. 1 and No. 2; the outputs of these are paralleled across a resistor which is very much smaller than the internal impedance of the output stages of the individual amplifiers. The pulses across this resistor are amplified and fed into a 20-channel pulse-height analyzer. The coincidence analyzer gates the pulse-height analyzer when there is a coincidence between pulses from amplifiers No. 1 and No. 2. When connected as shown in Fig. 1, the sum pulses are recorded; by breaking connections *A* (or *B*), the pulses from No. 2 (or No. 1) only are recorded. Accidentals are determined by throwing switch *S* to the left, which inserts a delay in channel No. 1. Tests showed that the accidental rate determination is not sensitive to the exact length of this delay.

The two detectors are balanced by adjusting the photomultiplier voltages to set the elastic-scattering peaks obtained without coincidence gating at the same channel. Tests with a pulser and with the coincidence protons from *p*-*p* scattering with and without absorbers indicated that there are no significant shifts from breaking connections *A* or *B*, and that the addition of pulses is linear. The variable delay is set by taking delay curves for *p*-*p* scattering. A typical set of curves, obtained with the polyethylene target and the detectors set a 45°L⁶ and 45°R, is shown in Fig. 2. To improve the energy resolution in these measurements, narrow

⁵ W. H. Jordan and P. R. Bell, Rev. Sci. Instr. 18, 703 (1947).

⁶ An L or R following an angle indicates the left or right side of the incident beam, respectively.

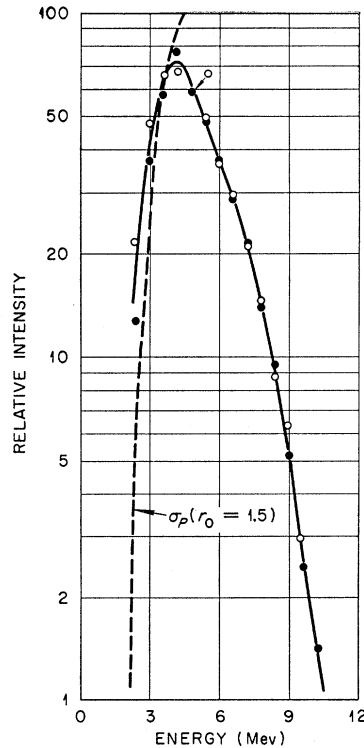


FIG. 3. Energy distribution of protons emitted in 23-Mev proton-induced $\text{Ni}^{58}(p,2p)$ reactions. Detection angles for this data were 90°L and 90°R , but data obtained at other angles were indistinguishable from this except for shifts due to center-of-mass motion. Each set of points represents an average of about twelve measurements. The dashed curve represents, essentially, the Coulomb barrier penetration factor for a nuclear radius of $1.5A^{1/3} \times 10^{-13}$ cm.

slits are placed in front of the detectors; the reduced energy is obtained with an absorber.

A large number of experimental difficulties were encountered in the course of this work. Some of them were:

(1) The pulses to the coincidence analyzer occur when the pulses in the amplifiers cross the discrimination level; this occurs at a later time for small pulses than for large pulses, thus explaining the shifting of the curves in Fig. 2. This effect can be very serious if proper precautions are not taken. To minimize it, it is necessary to use high amplifications and low discriminator settings on amplifiers No. 1 and No. 2, and to set the variable delay very accurately. Even so, it is probable that coincidences between a very large pulse and a very small pulse are missed in a small fraction of cases. Due to this problem, amplifications are not subject to major adjustments. In order to spread the interesting portion of the spectrum across the 20 channels, a voltage divider is used at the input to the pulse-height analyzer.

TABLE II. Detectors at 90° and 45° . Ratio of intensity with detectors 135° apart to intensity with detectors 45° apart.

Spectrum type	Position	$I(135^\circ \text{ apart})/I(45^\circ \text{ apart})$
Sum	$Q=0$	1.15 ± 0.08
Sum	$Q=-2.6$ Mev	1.14 ± 0.06
Sum	$Q=-4.7$ Mev	1.12 ± 0.06
Single	Peak	1.11 ± 0.05
Single	$E \sim 7$ Mev	1.22 ± 0.07

(2) Because of the low discriminator settings, gamma rays are also detected in the coincidence circuit. This proves especially difficult when the principal portion of the beam drifts away from the slit and strikes the collimator. In order to overcome this, an elaborate shielding system was developed. In addition, a scintillation counter was installed to determine the gamma-ray counting rate from the slit. The ratio of this rate to the proton counting rate was frequently minimized by adjusting the beam steering magnets to center the beam on the slit.

(3) The accidental rate was always very much higher than calculated. This is presumably due to the fact that a cyclotron is not a steady source. The well known rf pulsing is not responsible since the coincidence resolving time, $0.1 \mu\text{sec}$, is much longer than an rf period. A considerable effort was expended in changing cyclotron parameters to minimize this effect, but without notable success.

(4) Because of the long periods required to accumulate coincidence data, it was necessary to operate at total counting rates normally considered excessive (~ 1500 counts/sec). This resulted in shifting of pulse height vs energy curves, and in some loss of resolution. As angles are changed, it is, of course, impossible to maintain uniform total counting rates in both detectors; this accentuates the above problems.

These effects, coupled with the very steep energy dependence and the relatively small effects being studied, seriously decrease the accuracy of angular anisotropy measurements with pulse-height spectra from one detector only. This proved to be a major advantage of using sum spectra.

Data were obtained for each setting of the counters on two regular runs of about ten-minute duration each, with an accidental run sandwiched between. Accidental rates were corrected for the relative time of the runs for a given number of monitor counts. At the most intense parts of the spectra, true-to-accidental ratios of about 4:1 were commonly obtained. All data were taken in series of runs in which left and right sides were interchanged and the two counters were interchanged, so that alignment errors are canceled out. In all, the experiment included many hundreds of measurements of spectra.

The effect of gammas from the target in true coincidence with protons was studied by using absorbers, and their effect was found to be negligible. The crystals

TABLE III. Detectors at 90° and 135° . Ratio of intensity with detectors 135° apart to intensity with detectors 45° apart.

Spectrum type	Position	$I(135^\circ \text{ apart})/I(45^\circ \text{ apart})$
Sum	$Q=0$	1.19 ± 0.08
Sum	$Q=-2.6$	1.15 ± 0.05
Sum	$Q=-4.7$	1.13 ± 0.05
Single	Peak	1.16 ± 0.05
Single	$E \sim 7$ Mev	1.24 ± 0.07

are sufficiently thin that their efficiency for detecting gammas is only a few percent.

RESULTS

Figure 3 shows the energy distribution of the protons detected at 90°R in coincidence with protons at 90°L (and vice versa). This energy distribution was found to be essentially independent of either the angle of the detector or the coincidence detector; with the exception of small energy shifts explainable as center-of-mass effects, changes in these angles were reflected only in changes in over-all intensity. The high-energy portion of the spectrum exhibits a very rapid decrease in intensity with increasing energy; making corrections for Coulomb barrier penetration and energy gives a slope corresponding to a nuclear temperature of 0.9 Mev. This is considerably steeper than the spectrum obtained by Gugelot⁷ ($T \approx 1.5$ Mev) from inelastic scattering of 18-Mev protons by nickel. The low-energy portion of the observed spectrum is featured by a very sharp decrease due to the Coulomb barrier; the calculated barrier-penetration factor (using $r_0 = 1.5 \times 10^{-13}$ cm) is shown in the figure.

Figure 4 shows the distribution of the sum of the energies of the two protons. The data shown were obtained with the detectors at 90°L and 90°R, but here again, the shape of the distribution was essentially independent of the detector angles. One small exception to this is that the dip at about 9.5 Mev seems to be somewhat less pronounced, although still present, when the detectors are at backward angles. Another possible exception is in the height of the peak at 13.7 Mev relative to the rest of the spectrum; there is some evidence (see Tables II, III, and IV) for slight variations in this.

The peak at 13.7 Mev in Fig. 4 corresponds to the final nucleus, Co⁵⁷, being left in its ground state. The calculated value for this energy is 13.7 ± 0.2 Mev, in excellent agreement with the observation. Approximately 11% of the area under the curve is contained under this peak. A steep rise is observed leading to the calculated position of the first two excited states of Co⁵⁷ at $-Q = 1.4$ and 1.5 Mev; although these groups are not resolved, the shape indicates that the area under these peaks is somewhat larger than that under the ground state peak. Taken together, the area under these three peaks represents about 25% of the total

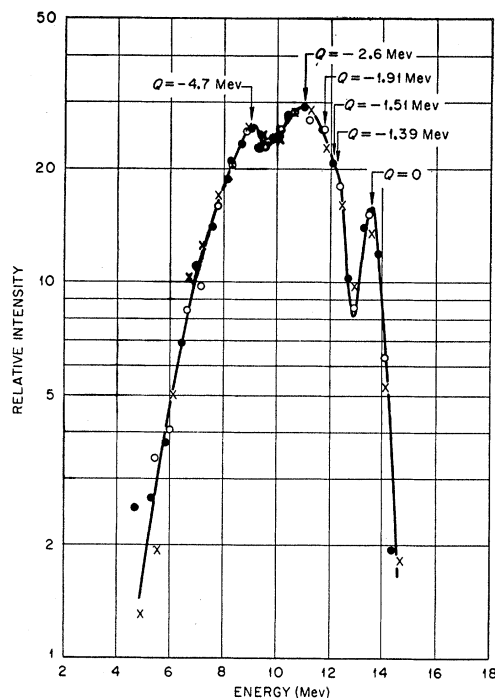


FIG. 4. Distribution of the sum of the energies of the two protons emitted in Ni($p, 2p$) reactions. Detection angles for this data were 90°L and 90°R, but data obtained at other angles were essentially indistinguishable from this except for shifts due to center-of-mass motion. Each set of points represents an average of about seven measurements.

area under the spectrum. The other features of Fig. 4 are broad peaks at $Q = -2.6$ Mev and $Q = -4.7$ Mev with a definite dip between.

The major angular distribution effort was directed toward measuring azimuthal anisotropies; that is, differences in the intensity between two positions in which the detectors are at the same angle relative to the incident beam, but at different angles relative to each other. The results are summarized in Tables II and III. They show that there is quite definitely an azimuthal anisotropy; it shows no strong energy dependence; and for the cases studied, namely 135° separation vs 45° separation, the probability of the larger separation is about 17% higher. A special set of detectors was constructed allowing a few measurements to be made with separations as small as 20°; there was no marked change in the azimuthal anisotropy.

The one systematic difference between the runs with detectors 135° apart and 45° apart is that in the former case, the detectors view opposite sides of the target, whereas in the latter they view the same side. In order to check for spurious effects due to this, a 0.6-mg/cm² target (one-fourth as thick as the usual one) was installed; again there was no marked change in the azimuthal anisotropy.

A lesser effort was expended in studying the angular distribution of the outgoing protons relative to the

TABLE IV. Ratio of intensity with detectors at various angles.

Spectrum type	Position	35°L-35°R	35°L-135°L	35°L-35°R
		35°L-135°L	135°L-135°R	135°L-135°R
Sum	$Q=0$	1.28	1.12	1.43
Sum	$Q=-2.6$ Mev	1.08	1.20	1.29
Sum	$Q=-4.7$ Mev	1.12	1.14	1.28

⁷ P. C. Gugelot, Phys. Rev. **93**, 425 (1954).

TABLE V. Angular distribution of second detector with first detector at 90° (sum spectrum, $-Q=2$ to 5 Mev).

Angle of second detector	Relative intensity
45°	1.16±0.10
90°	1.04±0.10
135°	1.00

incident protons. Some of the results are shown in Tables IV and V. They indicate that intensities are higher in the forward direction, although the anisotropy is not large.

CONCLUSIONS AND DISCUSSIONS

The most important problem to be investigated in the light of these results is the explanation for the strange preponderance of $(p,2p)$ over (p,pn) reactions in Ni⁵⁸. It may be hoped that this will elucidate the much broader problem of the general preponderance of proton emission over neutron emission in this mass region.

Some of the more usual explanations of this effect as applied to the present problem are:

- (1) The first emitted proton comes off with very high energy so that there is insufficient energy available for a neutron to be emitted as the second particle.
- (2) The Coulomb barrier is not very effective in impeding proton emission.⁸
- (3) The level density of Co⁵⁷ is very much larger than the level density of Ni⁵⁷, so that the former is favored statistically.³
- (4) The states of Co⁵⁷ have a higher fractional parentage of the original nucleus, Ni⁵⁸, than do the states of Ni⁵⁸.
- (5) The incident particle, which in this case is a proton, has a high probability of being re-emitted.

Item (1) can readily be seen to be incorrect from Fig. 3. Only if the first proton is emitted with an energy greater than 9.9 Mev is neutron emission energetically forbidden; this occurs in only about 1% of all reactions. Most protons come off with less than 6 Mev, leaving at least 4 Mev available for neutron emission.

Item (2) is also refuted by Fig. 3. The proton energy spectrum drops off sharply below the Coulomb barrier in approximately the expected manner.

Item (3), the level-density argument, is perhaps the most widely used explanation for this effect. However, Fig. 4 indicates that level densities have little to do with the matter. For example, 11% of all $(p,2p)$ reactions go to the ground state of Co⁵⁷, and an equal number goes to its first two excited states. There are, thus, as many $(p,2p)$ reactions going to the lowest three states of Co⁵⁷ as there are (p,pn) reactions in toto.

⁸ D. L. Hill and J. A. Wheeler, Phys. Rev. **89**, 1102 (1953).

A simple calculation (see Appendix A) shows that there should actually be more (p,pn) reactions going to the ground and first excited states of Ni⁵⁷ alone. This leaves no (p,pn) cross section from competition with the other 75% of $(p,2p)$ reactions, whereas statistical theory⁹ predicts that (p,pn) reactions should be favored over these by a factor of two.

Another argument against the importance of level densities arises from comparing the relative probabilities of $(p,2p)$ reactions going to the ground and excited states of Co⁵⁷. High-resolution measurements of even low-energy inelastic scattering¹⁰ have revealed forty levels in Co⁵⁹ from 1.0- to 3.7-Mev excitation. It thus seems certain that many hundreds of excited states of Co⁵⁷ can be reached by $(p,2p)$ reactions without undue impedance from Coulomb barrier effects. The fact that one reaction in nine goes to the ground state indicates that level densities do not have a controlling influence over the situation. Level density arguments would also not be able to account for the peaks at 2.6 and 4.7 Mev in Fig. 4.

Item (4), the fractional parentage argument, is impossible to refute in complete detail because of lack of knowledge. It is difficult, however, to see why the original nucleus, Ni⁵⁸, should have a larger fractional parentage of Co⁵⁷ (ground state) corresponding to a proton withdrawn from its closed shell, than of Ni⁵⁷ (ground state) which has only a neutron removed from an open shell. Moreover, the excessive emission of protons seems to be so general throughout this mass region that it is most unlikely that it can be attributed to the properties of specific nuclear states.

Item (5) seems to be an attractive explanation for the fact that (p,pn) reactions are usually the predominant reaction in this mass region. It does not explain the remaining cases where $(p,2p)$ reactions predominate; however, in every case of this type, the latter reaction is energetically favored. While there is no obvious explanation why this energetic favoring should have such a large influence, it is not inconceivable that it might.

Another difficulty with explaining the high probability for proton emission as reemission of the incident proton is that (α,pn) reactions have also been found⁸ to be very large. However, Weisskopf has pointed out¹¹ that there is probably not much connection between proton- and alpha-particle-induced reactions since the latter are very probably "stripping" processes.

Another important problem is to determine the reaction mechanism in the reaction under study. The two mechanisms which seem worthy of consideration are:

⁹ J. M. Blatt and V. F. Weisskopf, *Theoretical Nuclear Physics* (John Wiley and Sons, Inc., New York, 1952).

¹⁰ Mazari, Sperduto, and Buechner, Bull. Am. Phys. Soc. Ser. II, **2**, 179 (1957).

¹¹ V. F. Weisskopf (private communication).

(a) inelastic proton scattering followed by proton boil-off;

(b) direct interaction in which both particles are "knocked-out" simultaneously.

The 17% azimuthal anisotropy indicates that at least this fraction of the reactions proceeds by mechanism (b); the fact that the energy distributions are so independent of angle strongly suggests that this fraction is much higher. The fact that level densities play such an unimportant role in determining the course of the reaction argues very strongly against mechanism (a). The shape of the sum spectrum, Fig. 4, is typical of direct interaction spectra¹²; the peaks at $-Q=2.6$ and 4.7 Mev would be essentially impossible to explain with a "boil-off" theory.

There thus seems to be very strong evidence that the reaction mechanism is predominantly a direct interaction. The fact that the incident particle seems to be re-emitted indicates that there is only a single, or at most, only a few collisions.

ACKNOWLEDGMENTS

The author is greatly indebted to S. W. Mosko and F. A. DiCarlo for their help in data recording, to G. G. Kelly for discussion of electronic arrangements, to H. G. Blosser for help in designing and building the scattering chamber, and to V. F. Weisskopf for very helpful discussions. The support and encouragement of R. S. Livingston and A. M. Weinberg are gratefully acknowledged.

APPENDIX A. CALCULATION OF RELATIVE PROBABILITY FOR (*p,pn*) REACTIONS TO THE LOWEST STATES OF Ni⁵⁷ AND (*p,2p*) REACTIONS TO LOWEST STATES OF Co⁵⁷

We designate (*p,pn*) reactions to the ground and first excited state of Ni⁵⁷ as N_1 and N_2 , respectively, and (*p,2p*) reactions to the ground and first two excited

¹² B. L. Cohen, Phys. Rev. **105**, 1549 (1957); B. L. Cohen and S. W. Mosko, Phys. Rev. **106**, 995 (1957).

states of Co⁵⁷ as P_1 , P_2 , and P_3 , respectively. The cross section for any reaction is proportional to⁹ the energy of the outgoing particle, E , times the cross section for the inverse process, σ_i . The most favorable assumption is that the highest energy protons in the spectrum, Fig. 3, are accompanied by proton emission to give P_1 . Since 11% of all (*p,2p*) reactions are P_1 , this must be true of the uppermost 5.5% of the spectrum, which includes all protons above 8.0 Mev; the mean energy is 8.7 Mev. Thus, the competition between P_1 and N_1 is between emission of a 5.1-Mev proton and a 1.1-Mev neutron. The E factor favors proton emission by a factor of 4.6, but the σ_i factor favors neutron emission by a factor of 7. Thus

$$\sigma(P_1) \simeq 0.66\sigma(N_1). \quad (1)$$

Using the same calculation on the remaining protons in the spectrum, the competition between N_1 and P_2 or P_3 is between emission of 5.0-Mev protons and 2.5-Mev neutrons. The result is

$$\sigma(P_2) \simeq \sigma(P_3) \simeq 0.27\sigma(N_1). \quad (2)$$

Adding each of (2) to (1) gives

$$\sigma(P_1) + \sigma(P_2) + \sigma(P_3) \simeq 1.2\sigma(N_1). \quad (3)$$

If the first excited state of Ni⁵⁷ were at 2.0 Mev, the competition between N_2 and P_2 or P_3 would yield

$$\sigma(P_2) \simeq \sigma(P_3) \simeq 1.4\sigma(N_2). \quad (4)$$

Adding (1), 0.63 times each of (2), and 0.37 times each of (3) gives

$$\sigma(P_1) + \sigma(P_2) + \sigma(P_3) = \sigma(N_1) + \sigma(N_2). \quad (5)$$

Experimentally, the left sides of (3) and (5) are equal to the entire (*p,pn*) cross section. Therefore, competition from the ground state of Ni⁵⁷ should account for 83% of this, and if Ni⁵⁷ has even one excited state below 2 Mev—a virtual certainty—there is already a discrepancy. Furthermore, there is no (*p,pn*) cross section left to account for the competition with the remaining 75% of (*p,2p*) reactions.